



Published in final edited form as:

Cancer Cell. 2010 August 9; 18(2): 185–197. doi:10.1016/j.ccr.2010.06.016.

Regulation of Tumor Angiogenesis by EZH2

Chunhua Lu^{1,*}, Hee Dong Han^{1,*}, Lingegowda S. Mangala^{1,*}, Rouba Ali-Fehmi², Christopher S. Newton³, Laurent Ozbun³, Guillermo N. Armaiz-Pena¹, Wei Hu¹, Rebecca L. Stone¹, Adnan Munkarah⁴, Murali K. Ravoori⁵, Mian M. K. Shahzad^{1,6}, Jeong-Won Lee^{1,7}, Edna Mora^{1,8}, Robert R. Langley⁹, Amy R. Carroll¹, Koji Matsuo¹, Whitney A. Spannuth¹, Rosemarie Schmandt¹, Nicholas B. Jennings¹, Blake W. Goodman¹, Robert B. Jaffe¹⁰, Alpa M. Nick¹, Hye Sun Kim^{1,11}, Eylem Ozturk Guven¹², Ya-Huey Chen¹³, Long-Yuan Li¹⁴, Ming-Chuan Hsu¹⁵, Robert L. Coleman^{1,16}, George A. Calin^{16,17}, Emir B. Denkbaz¹², Jae Yun Lim¹⁸, Ju-Seog Lee¹⁸, Vikas Kundra⁵, Michael J. Birrer¹⁹, Mien-Chie Hung^{13,15}, Gabriel Lopez-Berestein^{9,16,17}, and Anil K. Sood^{1,9,16,20}

¹ Department of Gynecologic Oncology, U.T. M.D. Anderson Cancer Center, 1155 Herman Pressler, Unit 1362, Houston, TX 77030

² Department of Pathology, Wayne State University School of Medicine, Karmanos Cancer Institute, Detroit, MI 48201

³ Department of Cell and Cancer Biology, National Cancer Institute, Bethesda, MD 20892

⁴ Women's Health Services, Henry Ford Health System, Detroit, MI 48202

⁵ Department of Experimental Diagnostic Imaging, U.T. M.D. Anderson Cancer Center, 1515 Holcombe Blvd, Unit 368, Houston, TX 77030

⁶ Baylor College of Medicine, Department of Obstetrics and Gynecology, Houston, TX 77030

⁷ Department of Obstetrics and Gynecology, Samsung Medical Center, Sungkyunkwan University School of Medicine, Seoul, Korea 135-710

⁸ Department of Surgery, University of Puerto Rico, San Juan, PR 00935

⁹ Department of Cancer Biology, U.T. M.D. Anderson Cancer Center, 1515 Holcombe Boulevard, Houston, TX 77030

¹⁰ Center for Reproductive Sciences, 505 Parnassus, University of California, San Francisco, CA 94143

¹¹ Department of Pathology, Cheil General Hospital and Women's Healthcare Center, Kwandong University College of Medicine, Seoul, Korea 100-380

¹² Hacettepe University, Nanotechnology and Nanomedicine Division, Ankara, Turkey 06532

¹³ Center for Molecular Medicine, China Medical University and Hospital, Taichung, Taiwan 404

²⁰Correspondence and Reprint Requests: Anil K. Sood, Professor, Departments of Gynecologic Oncology and Cancer Biology, The University of Texas, M.D. Anderson Cancer Center, 1155 Herman Pressler, Unit 1362, Houston, TX 77030 Phone: 713-745-5266, Fax: 713-792-7586, asood@mdanderson.org.

*These authors contributed equally to this work

Accession number.

The microarray data have been deposited into NCBI GEO (Accession ID, GSE20381).

Publisher's Disclaimer: This is a PDF file of an unedited manuscript that has been accepted for publication. As a service to our customers we are providing this early version of the manuscript. The manuscript will undergo copyediting, typesetting, and review of the resulting proof before it is published in its final citable form. Please note that during the production process errors may be discovered which could affect the content, and all legal disclaimers that apply to the journal pertain.

¹⁴ Graduate Institute of Cancer Biology, China Medical University and Hospital, Taichung, Taiwan 404

¹⁵ Department of Cellular and Molecular Oncology, U.T. M.D. Anderson Cancer Center, 1515 Holcombe Blvd, Unit 950, Houston, TX 77030

¹⁶ Center for RNAi and Non-Coding RNA, U.T. M.D. Anderson Cancer Center, 1515 Holcombe Blvd, Unit 950, Houston, TX 77030

¹⁷ Department of Experimental Therapeutics, U.T. M.D. Anderson Cancer Center, 1515 Holcombe Blvd, Unit 950, Houston, TX 77030

¹⁸ Department of Systems Biology, U.T. M.D. Anderson Cancer Center, 1515 Holcombe Blvd, Unit 950, Houston, TX 77030

¹⁹ Department of Medicine, Harvard Medical School, Massachusetts General Hospital Cancer Center, Boston, MA 02114

SUMMARY

While VEGF-targeted therapies are showing promise, new angiogenesis targets are needed to make additional gains. Here, we show that increased *Zeste* homologue 2 (EZH2) expression in either tumor cells or in tumor vasculature is predictive of poor clinical outcome. The increase in endothelial EZH2 is a direct result of VEGF stimulation by a paracrine circuit that promotes angiogenesis by methylating and silencing vasohibin1 (VASH1). EZH2 silencing in the tumor-associated endothelial cells inhibited angiogenesis mediated by reactivation of VASH1, and reduced ovarian cancer growth, which is further enhanced in combination with EZH2 silencing in tumor cells. Collectively, these data support the potential for targeting EZH2 as an important therapeutic approach.

SIGNIFICANCE

In this work, we identify EZH2 as a key regulator of tumor angiogenesis. The increase in endothelial EZH2 is a direct result of VEGF stimulation and indicates the presence of a paracrine circuit that promotes angiogenesis. EZH2 silencing in the tumor-associated endothelial cells using siRNA, packaged in the chitosan delivery system, resulted in significant growth inhibition in an orthotopic ovarian cancer model. EZH2 silencing in tumor endothelial cells resulted in decreased angiogenesis that was mediated by increased levels of the angiogenesis inhibitor, vasohibin1 (VASH1). Combined, these data provide a significant conceptual advance in our understanding of the regulation of angiogenesis in ovarian carcinoma and support the potential for targeting EZH2 as a therapeutic approach.

Keywords

RNA interference; EZH2; chitosan; ovarian carcinoma

INTRODUCTION

Targeting the tumor vasculature is a particularly attractive strategy because of the presumed genetic stability of endothelial cells (Folkman, 1990). Anti-angiogenic therapeutic strategies are predicted to be meritorious in ovarian cancer patients based on tumor and endothelial VEGF overexpression, and response characteristics noted in phase II clinical trials (Burger et al., 2007; Jain et al., 2006; Spannuth et al., 2008). As such, 7 phase III clinical trials in primary and recurrent disease have completed enrollment or are accruing. However, despite initial responses, most patients eventually experience disease progression. The mechanism for this acquired resistance is not well described, but appears to be due in part to expansion

or expression of redundant (Relf et al., 1997) alterations in maturing vasculature (Huang et al., 2004) and epigenetic mechanisms (Kerbel, 2001a; Kerbel et al., 2001b); therefore, new anti-angiogenesis targets are needed.

In search of such targets, we carried out genomic profiling studies of endothelial cells from epithelial ovarian cancer and from their normal counterparts (Lu et al., 2007a). Among the many genes with increased expression in tumor endothelial cells, we focused on the enhancer of Zeste homologue 2 (EZH2), a member of the polycomb-group (PcG) proteins. PcG proteins are negative regulators of gene expression and are involved in the stable transmission of the repressive state of their target gene throughout the cell cycle (Cavalli and Paro, 1998; Kingston et al., 1996; Simon, 1995). EZH2, a critical component of the polycomb repressive complex 2 (PRC2), has intrinsic histone methyl transferase (HMTase) activity and has been implicated in the progression and metastasis of several cancers (Cha et al., 2005; Raman et al., 2005). For instance, normalized EZH2 mRNA transcripts were significantly associated with invasiveness of bladder tumors and were significantly higher in grade 3 *versus* grade 1 and 2 tumors (Weikert et al., 2005). Similar relationships have been described in breast (Kleer et al., 2003), prostate (Varambally et al., 2002), gastric (Matsukawa et al., 2006) and squamous cell cancers of the oral pharynx (Kidani et al., 2009). The association of EZH2 with the malignant phenotype of many solid tumors and its function as a repressor of gene targets led to the hypothesis that EZH2 could impact specific angiogenic mechanisms of endothelial cell biology. Herein, we focused on EZH2 mediated regulation of vasohibin1 (VASH1), which is an endothelial cell specific and intrinsic negative regulator of angiogenesis (Hosaka et al., 2009; Watanabe et al., 2004).

RESULTS

EZH2 expression in human ovarian carcinoma

We first examined the clinical significance of EZH2 in 180 epithelial ovarian cancers. Increased tumoral EZH2 (EZH2-T) expression, based on the histochemical score, was noted in 66% of samples and increased expression in the vasculature (EZH2-Endo) was noted in 67% of the samples (Figures 1A and 1C). Increased expression of EZH2-T and EZH2-Endo was significantly associated with high-stage ($p < 0.001$) and high-grade ($p < 0.05$; Table 1) disease. Increased EZH2-T was significantly associated with decreased overall survival (median 2.5 years vs. 7.33 years, $p < 0.001$; Figure 1B). Similarly, EZH2-Endo was predictive of poor overall survival (2.33 vs. 8.33 years, $p < 0.001$; Figure 1D). On the basis of pathway-analysis predictions from our genomic profiling data comparing endothelial cells from epithelial ovarian cancer with those from normal ovarian tissues (Lu et al., 2007a), we next examined potential associations between EZH2 and VEGF expression, and microvessel density (MVD). Tumors with increased VEGF expression had significantly greater prevalence of increased EZH2-Endo expression ($p < 0.001$; Figures 1E and 1F). Moreover, tumors with increased EZH2-Endo expression had significantly greater MVD ($p < 0.001$ by Wilcoxon ranked sums test; Figures 1G and 1H).

VEGF increases EZH2 levels in endothelial cells

On the basis of our observations from clinical samples, we next asked whether VEGF could directly regulate EZH2 levels in endothelial cells. For these experiments, mouse ovarian endothelial cells (MOEC) were co-transfected with the Renilla luciferase plasmid and firefly luciferase plasmid either with or without the EZH2 promoter construct. Cells were then treated with VEGF, or conditioned media from SKOV3 ovarian cancer cells (SKOV3-CM). There was a significant increase in EZH2 promoter activity in endothelial cells in response to VEGF, and conditioned media (Figure 1I). To examine changes in EZH2 message, MOECs were treated as indicated above and EZH2 mRNA was quantified using real time

RT-PCR. EZH2 mRNA expression levels were significantly increased in endothelial cells in response to VEGF, or SKOV3-CM (Figure 1I). The increases in EZH2 promoter activity and mRNA levels in response to SKOV3-CM or VEGF were blocked with the VEGFR2 specific antibody DC101. Similarly, increased EZH2 protein levels in response to VEGF were blocked by the anti-VEGFR2 antibody (Figure S1A).

Since EZH2 levels were noted to be increased in tumor and tumor-associated endothelial cells, we next asked whether there was a correlation between the two compartments in human ovarian carcinoma. Orthogonal regression modeling between these factors described a high coefficient of correlation ($r=0.83$, $p < 0.001$; Figure S1B). To address whether tumor derived VEGF affected endothelial EZH2, we utilized an orthotopic model of ovarian cancer metastasis. SKOV3ip1 tumor bearing animals were treated with either control antibody or bevacizumab (selective for human VEGF). Following treatment for 2 weeks, the tumors were harvested and tumor and endothelial cells were isolated. Compared to normal endothelial cells, EZH2 levels were significantly higher in the tumor endothelial cells, and this increase was substantially reduced in the bevacizumab treated samples (Figure S1C). Conversely, bevacizumab had no effect on tumor cell EZH2 levels (Figure S1D). To examine for direct effects of EZH2 on endothelial cells, we transfected EZH2 into MOEC, and examined for effects on tube formation using *in vitro* assays. Compared to empty vector controls, EZH2 promoted tube formation ($p < 0.01$), which was only minimally blocked by a VEGFR2 inhibitor (Figure S1E). Similar results were noted with HUVECs (data not shown).

EZH2 silencing increases VASH1 in endothelial cells

To determine the mechanism by which EZH2 could promote angiogenesis, we searched a database from a whole genome CHIP-on-CHIP analysis that was performed in a separate study. We found that an anti-angiogenic gene, VASH1, directly binds to EZH2. To validate this finding, we performed a CHIP assay of EZH2 for the VASH1 promoter in endothelial cells in the presence or absence of VEGF (Figure 2A), which confirmed direct EZH2 binding to the VASH1 promoter. Quantitative CHIP analysis confirmed the enhanced binding of EZH2 to the VASH1 promoter in response to VEGF (Figure 2B). Next, we silenced the EZH2 gene in MOECs using two different siRNA sequences (Figure 2C), which resulted in a 3.6-3.8 fold increase in VASH1 (Figure 2D). Moreover, there was a significant increase in VASH1 promoter activity following EZH2 gene silencing (Figure S2).

To determine the mechanism by which EZH2 regulates VASH1, we performed methylation specific PCR to detect VASH1 methylation in endothelial cells in the presence of VEGF after silencing EZH2. We found that VEGF treatment resulted in a 1.7 fold increase in VASH1 methylation compared to the controls (Figure 2E). However, EZH2 silencing resulted in a 3.3 fold decrease in VASH1 methylation in the VEGF-treated MOECs. EZH2 gene silencing also decreased histone 3 methylation at lysine 27 by 2.5-fold in endothelial cells (Figure 2F).

E2F mediated regulation of EZH2 in endothelial cells

It is known that VEGF can activate E2F transcription factors (Zhu et al., 2003). Due to their suspected role in regulating EZH2 levels, we first tested the effect of VEGF on E2F1-5 in MOECs. There was a significant increase in E2F1 and E2F3, but not others, following treatment with VEGF (Figure 3A). To determine which E2F transcription factors might be responsible for increasing EZH2 levels, we next examined the effects of VEGF after silencing either E2F1 or 3. EZH2 levels were significantly decreased in E2F1 and E2F3 silenced cells (Figure 3B). To validate the binding of EZH2 promoter to E2F1 and/or E2F3

transcription factors, we performed ChIP assays of EZH2 to these transcription factors. As shown in Figure 3C, E2F1 and E2F3 bind directly to the EZH2 promoter, demonstrating that EZH2 is a direct target of the E2F transcription factors (Wu et al., 2010). Moreover, the VEGF mediated binding of EZH2 to the VASH1 promoter was abrogated with E2F1 or E2F3 gene silencing (Figure 3D).

To determine the functional role of VASH1 in angiogenesis, we performed migration and tube formation assays using MOECs following VASH1 gene silencing using two different siRNA sequences. Both cell migration and tube formation were significantly increased after VASH1 gene silencing (Figures S3A and S3B). Similar results were obtained with HUVEC (data not shown).

***In vivo* EZH2 gene silencing**

On the basis of our *in vitro* findings, we next asked whether EZH2 gene silencing *in vivo* would affect tumor growth and angiogenesis. Before conducting the EZH2 targeted *in vivo* experiments, we developed and characterized chitosan (CH) nanoparticles for systemic delivery of siRNA into both tumor cells and tumor-associated vasculature. Several formulations of CH with siRNA (siRNA/CH) were tested (Figure S4A) and optimized (Figures S4B-S4I) and the 3:1 ratio (CH:TPP) nanoparticles showed the greatest (75%) incorporation efficiency (Figure S4D). Therefore, for all subsequent experiments, we used the siRNA/CH3 nanoparticles due to their small size, slight positive charge, and high incorporation efficiency of siRNA.

Prior to performing proof-of-concept *in vivo* efficacy studies, we tested the efficiency of siRNA delivery into orthotopic ovarian tumors. Non-silencing siRNA labeled with Alexa-555 was incorporated into CH nanoparticles and injected intravenously (i.v.) into mice bearing HeyA8 orthotopic tumors (17 days after intraperitoneal (i.p.) inoculation of tumor cells). Tumors were harvested at 15 hours and 3, 5 or 7 days (3 mice per time point) following injection and examined for extent of siRNA delivery. At all time points, punctated emissions of the siRNA were noted in the perinuclear regions of individual cells. SiRNA was noted in >80% of fields examined following a single intravenous injection. To confirm delivery of siRNA in the vasculature, slides were also stained for CD31. Indeed, siRNA was delivered into the tumor-associated endothelial cells, suggesting potential applications for targeting the tumor vasculature (Figure 4A). To confirm intracellular delivery of siRNA, we created 3-dimensional reconstructions of the tumors using confocal microscopy. Lateral views of the optical sections clearly demonstrated the presence of siRNA within the tumor cells (Figure 4B). However, very little siRNA was taken up by macrophages as determined by labeling tissues with f4/80 (Figure S4J).

To examine the biodistribution of siRNA into other organs, sections of liver, lung, kidney, heart, spleen and brain were also examined, and siRNA delivery was detected in most of these organs (Figure S4K). We also utilized optical imaging to assess biodistribution. Fluorescence corresponding to siRNA uptake was seen in tumor and various organs, such as kidney, liver, lung, and spleen (Figure 4C). Semi-quantitative assessment of fluorescence confirmed increased uptake of siRNA in HeyA8 tumors and various organs in mice injected intravenously with Cy 5.5 labeled siRNA/CH compared to those injected with unlabeled siRNA/CH (Figure 4D). To examine the *in vivo* effects of EZH2 gene silencing on tumor growth, we utilized EZH2 siRNA directed to either the human (tumor cells; EZH2 Hs siRNA/CH) or mouse (endothelial cells; EZH2 Mm siRNA/CH) sequence. The expression levels of EZH2 in ovarian cancer cells are shown in Figure S5A; the specificity of siRNA was confirmed by testing each siRNA in both MOEC and human tumor (HeyA8) cells (Figure S5B). Following intravenous injection of either control siRNA/CH, EZH2 Hs siRNA/CH, EZH2 Mm siRNA/CH, or the combination of EZH2 targeted siRNAs into

HeyA8 tumor-bearing mice (n=3 mice per group at each time point), tumors were harvested at different time points and examined for EZH2 protein levels. EZH2 levels were decreased by 24 hours following single injection of EZH2 Hs siRNA/CH with return of expression to baseline expression levels after 96 hours (Figure 5A). EZH2 gene silencing was also confirmed with real-time RT-PCR analysis of tumor and endothelial cells (Figure S5D and S5E).

To determine the localization of EZH2 silencing following siRNA/CH administration, we performed dual immunofluorescence staining for EZH2 and CD31. This experiment further demonstrated that EZH2 Hs siRNA/CH resulted in EZH2 silencing in the tumor cells whereas EZH2 Mm siRNA/CH silenced EZH2 only in the tumor endothelial cells (Figure 5B). To determine the therapeutic efficacy of EZH2 gene silencing, a well-characterized orthotopic model of ovarian carcinoma was utilized. Seven days following injection of tumor cells into the peritoneal cavity, mice were randomly allocated to one of the following groups (n=10 mice per group): 1) control siRNA/CH, 2) EZH2 Hs siRNA/CH, 3) EZH2 Mm siRNA/CH and 4) combination of EZH2 Hs siRNA/CH plus EZH2 Mm siRNA/CH. Mice were sacrificed when animals appeared moribund due to significant tumor burden (4 to 5 weeks after cell injection depending on the cell line). As shown in Figure 5C and Figure S5C, in both models, treatment with EZH2 Mm siRNA/CH resulted in a significant decrease in tumor burden compared to control siRNA/CH (62% reduction in HeyA8; $p < 0.02$ and 40% reduction in SKOV3ip1, $p < 0.03$). EZH2 Hs siRNA/CH as a single-agent had modest effects on tumor growth ($p < 0.04$ for HeyA8; and $p = 0.18$ for SKOV3ip1) compared with control siRNA/CH. However, the greatest reduction was observed with the combination of EZH2 Hs siRNA/CH plus EZH2 Mm siRNA/CH (83% reduction in HeyA8, $p < 0.001$ and 65% reduction in SKOV3ip1, $p < 0.001$). To test for potential off-target effects, we tested the efficacy of 3 additional mouse EZH2 siRNA sequences with similar effects on tumor growth (data not shown).

To evaluate the effects of EZH2 on other parameters of tumor growth, we examined tumor incidence and number of nodules (Table S1). The combination of EZH2 Hs siRNA/CH plus EZH2 Mm siRNA/CH resulted in a significant reduction in tumor nodules in both HeyA8 ($p = 0.002$ vs. control siRNA/CH treated group) and SKOV3ip1 tumors ($p = 0.004$ vs. control siRNA/CH treated group). The decrease in tumor burden occurred despite having comparable tumor incidence. The mean mouse body weight was similar among the different groups (data not shown), suggesting that feeding and drinking habits were not affected.

Effect of EZH2 targeting on tumor vasculature and proliferation

To identify potential mechanisms underlying the efficacy of EZH2 silencing on ovarian tumors, we examined its effects on several biological end points including MVD, pericyte coverage (desmin) and cell proliferation (PCNA). EZH2 Mm siRNA/CH and the combination therapy groups had significantly lower microvessel density (Figure 6A) compared to the EZH2 Hs siRNA/CH and control siRNA/CH treated SKOV3ip1 tumors. Pericyte coverage (assessed with desmin and alpha smooth muscle actin (ASMA) staining) was increased in EZH2 Mm siRNA/CH and the combination groups compared to other 2 groups, suggesting greater vascular maturation (Figure 6A and Figure S6B). Combination treatment with EZH2 Hs siRNA/CH and EZH2 Mm siRNA/CH also resulted in a significant reduction in cell proliferation (Figure S6C) and increased apoptosis (Figure S6C). Similar effects of EZH2 silencing on MVD, pericyte coverage, and proliferation were noted in the HeyA8 model (Figure S6D). To test the effect of EZH2 gene silencing on intratumor hypoxia, we measured viable hypoxic areas by staining tumor sections with pimonidazole. Compared to control siRNA/CH treated tumors, EZH2 Mm siRNA/CH treated tumors had modest increase in hypoxia (Figure S6E and S6F), which is consistent with effects of decreased angiogenesis.

VASH1 levels were significantly increased following EZH2 gene silencing in the tumor endothelial cells (Figure S6A). To determine the requirement for VASH1 in mediating the anti-tumor effects of EZH2 silencing, we examined the effects of VASH1 silencing in combination with EZH2 Mm siRNA/CH. The anti-tumor effect of EZH2 silencing in the tumor vasculature was completely reversed by VASH1 silencing (Figure 6B and Table S2), indicating that VASH1 is required for mediating the anti-tumor effects of EZH2 silencing.

To determine if endothelial EZH2 expression is related to VASH1 expression in human epithelial ovarian cancer, 37 samples were also immunostained for VASH1. The best-fit linear regression model demonstrated a significant inverse relationship ($R^2 = -0.59$; $p < 0.001$) between endothelial EZH2 and VASH1 scores (Figure 6C). Specifically, presence of high EZH2 expression was associated with low VASH1 expression, which was otherwise elevated in the absence of or in the presence of low EZH2 expression. We also examined mRNA levels of EZH2 and VASH1 in endothelial cells isolated from 3 normal ovarian and 10 epithelial ovarian cancer samples using quantitative RT-PCR. Compared to normal ovarian endothelial cells, VASH1 levels were significantly lower in samples with high *versus* low EZH2 levels (Figure 6D). To assess vessel maturation (pericyte coverage), the 37 human ovarian cancer samples were immunostained for ASMA. Tumors with low endothelial EZH2 had a significantly higher percentage of blood vessels with pericyte coverage ($p < 0.01$; Figure 6E).

To identify potential direct effects of EZH2 gene silencing on tumor cells, we performed a series of *in vitro* assays. EZH2 siRNA reduced migration by 64 to 71% ($p < 0.01$), and invasion by 63 to 72% ($p < 0.01$) in the SKOV3ip1 cells (Figures S5F-S5G). There were no significant effects on cell viability (Figure S5H). Similar results were noted with the HeyA8 cells (data not shown). To address the potential effects of tumor cell EZH2 gene silencing on invasion *in vivo*, we injected SKOV3ip1 tumor cells directly into the ovary and the animals were randomly allocated to the following groups ($n=10$ mice per group): 1) control siRNA/CH, 2) EZH2 Hs siRNA/CH. Following 4 weeks of treatment, the mice were dissected and the aggregate tumor weight was 30% lower ($p = 0.03$) in the EZH2 Hs siRNA/CH treated animals. While 50% of the mice in the control group developed para-aortic lymph node metastasis, none had nodal metastasis in the EZH2 Hs siRNA/CH group ($p < 0.001$). Moreover, the ovarian tumors in the control Hs siRNA/CH group had a more infiltrative growth pattern compared to the EZH2 Hs siRNA/CH group (Figure S5I). To identify genes potentially affected by EZH2 in ovarian cancer cells, we performed genomic analyses of SKOV3ip1 cells following treatment with either control or EZH2 siRNA. There were 788 genes with significantly increased or decreased expression (Figure S5J). Among these, gene networks of connective tissue growth factor (CTGF) were significantly reduced, which are known to regulate tumor cell migration and invasion (Figure S5K) (Chu et al., 2008; Cicha and Goppelt-Strube, 2009).

DISCUSSION

Our results describe a mechanism by which VEGF increases EZH2 levels in the tumor vasculature. EZH2, in turn, contributes to tumor angiogenesis by inactivating the anti-angiogenic factor, VASH1, by methylation. These results coupled with pathway-analysis predictions of genomic profiling data of tumor endothelial cells (Lu et al., 2007a) expand our understanding of tumor angiogenesis (Figure 7). Moreover, we have developed and characterized a highly effective method of gene silencing in tumor cells as well as in the blood vessels that support their growth.

PcG proteins play a critical role in determining cell fate during both normal and pathologic processes. Two separate subsets of PcG complexes (PRC1 and PRC2) have been described

in humans (Cao and Zhang, 2004). PRC1 is thought to be involved in maintenance of repression, whereas PRC2 plays a role in initiating repression. The PRC2 complex consists of the EZH2, EED, and SUZ proteins (Cao and Zhang, 2004). Altered expression of these proteins has been implicated in cancer pathogenesis (Raman et al., 2005; Cao and Zhang, 2004). However, prior to our work, the role of EZH2 in angiogenesis was not known.

Angiogenesis is regulated by the balance of various pro-angiogenic stimulators, such as VEGF, and several angiogenesis inhibitors such as angiostatin, and endostatin (Folkman, 1990). On the basis of findings from genomic profiling of endothelial cells from ovarian cancer *versus* those from normal ovaries, we discovered that EZH2 expression is significantly increased in tumor-associated endothelial cells (Lu et al., 2007a). VEGF is well recognized as a pro-angiogenic factor in ovarian and other cancers (Spannuth et al., 2008), and its receptors are expressed by endothelial and other cell types including tumor and perivascular cells (Spannuth et al., 2009). In the current study, we showed that VEGF can directly increase EZH2 levels in endothelial cells, which in turn inactivates a potent anti-angiogenic factor, VASH1. Silencing EZH2 gene resulted in demethylation of VASH1 in endothelial cells. This finding is consistent with the role of EZH2 in controlling DNA methylation of EZH2-targeted genes concomitant with reducing H3K27 (McGarvey et al., 2007). VASH1 is known to inhibit endothelial-cell migration, proliferation, and tube formation (Shen et al., 2006). VASH1 expression can be induced by VEGF as part of a negative feedback mechanism in endothelial cells (Hosaka et al., 2009; Tamaki et al., 2009; Watanabe et al., 2004; Yoshinaga et al., 2008). VASH1 limits tumor-associated angiogenesis and increases vessel maturity (Kern et al., 2009). Since VASH1 levels are low in the setting of high EZH2, VASH1 siRNA alone had no significant effect on tumor growth. However, VASH1 levels in tumor endothelial cells are increased in response to EZH2 gene silencing, and VASH1 siRNA blocked the inhibitory effects of EZH2 gene silencing on tumor growth.

A number of therapeutic anti-angiogenic targets have recently emerged supporting the clinical rationale of exploiting tumor and endothelial cell interactions. The most mature and promising among ovarian cancer patients involves VEGF and its receptors. For instance, bevacizumab, a chimeric monoclonal antibody targeting VEGF-A has demonstrated impressive single agent activity (objective response and non-progression at 6 months) in recurrent ovarian cancer patients and more recently, significant efficacy (PFS) in combination with chemotherapy administered in the frontline adjuvant setting (Burger et al., 2007; Burger et al., 2010). However, this compound and others in its class indiscriminately target VEGF, leading to a number of clinically significant and sometimes lethal side effects (Stone et al., 2010). In addition, new strategies targeting angiogenesis are needed as the above therapies are rarely curative and a growing population of patients are demonstrating VEGF resistance. EZH2 represents an innovative strategy, which has activity on both tumor cells and tumor-associated vasculature. The differential expression between normal and tumor vasculature may be hypothesized to have less off-target associated toxicity. Nevertheless, combinatorial approaches with VEGF targeting may augment efficacy and are attractive for further preclinical exploration.

While a number of important targets in tumor and endothelial cells have been identified, many of these are difficult to target with small molecule inhibitors and monoclonal antibodies. This limitation prompted us to utilize RNA interference as a means to target EZH2. We have recently demonstrated that a neutral nanoliposomal carrier allows efficient systemic delivery of siRNA into orthotopic tumors (Landen et al., 2005; Thaker et al., 2006). However, due to limited delivery of siRNA into the tumor-associated endothelial cells with this approach, we sought to develop additional nanoparticles that would allow siRNA delivery into both tumor and tumor-associated endothelial cells. Chitosan is desirable

for biological applications due to properties such as low immunogenicity and low toxicity (Kumar, 2000). These properties make use of chitosan for systemic *in vivo* siRNA delivery highly attractive (Howard et al., 2006). Indeed, our data demonstrate highly effective delivery of siRNA incorporated into chitosan nanoparticles into both tumor and tumor-associated endothelial cells. Such an approach may add a powerful tool to the armamentarium for targeting angiogenesis promoting genes.

In summary, molecular and genetic manipulations have identified EZH2 as a key regulator of tumor angiogenesis here, but these effects do not rule out the possibility that EZH2 has oncogenic functions in tumor cells (Cao and Zhang, 2004; Raman et al., 2005). For example, EZH2 has been implicated in cellular transformation, proliferation, and avoidance of apoptosis (Tonini et al., 2008). However, to the extent that targeting tumor endothelial cells provides therapeutic benefit (Burger et al., 2007; Jain et al., 2006), interfering with EZH2 in the tumor and endothelial cells might represent an important strategy for treatment of ovarian and other cancers.

EXPERIMENTAL PROCEDURES

Cell lines and culture

The HeyA8 and SKOV3ip1 human epithelial ovarian cancer cells were maintained as described previously (Kamat et al., 2007; Lu et al., 2007b). The derivation and characterization of the mouse ovarian endothelial cells (MOEC) has been described previously (Langley et al., 2003). HUVECs were purchased from Cambrex (Walkersville, MD) and maintained with heparin and gentamicin/amphotericin-B, as previously described (Ptasinska et al., 2007).

EZH2 promoter construct

The EZH2 promoter was amplified by PCR from the Roswell Park Cancer Institute human BAC library 11, Clone-ID RP11-992C19 purchased from the Children's Hospital Oakland Research Institute (Oakland, CA), and then cloned into the pGL3-Basic Vector (Promega Corp., Madison, WI). The EZH2 promoter construct was amplified using primers (see Supplemental Experimental Procedures) with XhoI and HindIII restriction endonuclease sites added to the ends. Purified PCR product was then cloned upstream of the luc⁺ gene in the pGL3-Basic Vector (Promega Corp.).

Luciferase reporter assay

Relative activity of the EZH2 promoter in MOEC was determined by luciferase reporter assays. Cells were transfected in low-serum medium (0.5% serum) with the firefly luciferase plasmid, either empty vector (pGL3-Basic) or the EZH2 promoter construct vector (EZH2prom-pGL3-Basic), in 12-well plates using Effectene[®] Transfection Reagent from Qiagen (Valencia, CA). Cells were then maintained in low-serum medium for 18 hours, washed in PBS, and treated in triplicate at 37°C for 6 hours. Treatments included recombinant human rhVEGF₁₆₅ (VEGF; 50 ng/mL; Peprotech, Rocky Hill, NJ), in fresh medium plus 0.5% serum, and conditioned media from immortalized ovarian surface epithelium (IOSE120) or SKOV3 ovarian cancer cells. Following treatment, cells were washed and processed using the Dual-Luciferase[®] Reporter Assay System (Promega Corp.).

Chromatin immunoprecipitation (ChIP) assay

Cells were cultured in low serum medium (0.5% serum) for 18 hours after being transfected with siRNA for 48 hours and then treated with or without VEGF (50 ng/mL) for 6 hours. After treatment, ChIP assays were performed using EZ ChIP[™] kit (Millipore, Temecula, CA) as described by the manufacturer. Briefly, cross-linked cells were collected, lysed,

sonicated and subjected to immunoprecipitation with EZH2 antibody (Cell signaling) or mouse IgG (mIgG) control. Immunocomplexes were collected with protein A/G agarose beads and eluted. Cross-links were reversed by incubating at 65°C. DNA was extracted and purified for PCR using primers (see Supplemental Experimental Procedures) corresponding to the 3800 to 3697 base pairs upstream of the VASH1 transcription start site.

Real time quantitative RT-PCR

Cells were seeded at 1.0×10^4 cells per well in 96-well plates in complete medium and incubated at 37°C for 24 hours, and then in low-serum medium (0.5% serum) for 18 hours, minus EGF and VEGF supplements where appropriate. Real-time quantitative RT-PCR was performed using 50 ng total RNA isolated from treated cells using the RNeasy Mini Kit (Qiagen). Relative expression values were obtained using the average of three reference genes and the $2^{\Delta\Delta CT}$ method as described previously, and normalized to control for percent fold changes (Donninger et al., 2004).

SiRNA constructs and delivery

SiRNAs were purchased from Qiagen, Dharmacon (Chicago, IL) or Sigma-Aldrich (Woodlands, TX). A non-silencing siRNA that did not share sequence homology with any known human mRNA based on a BLAST search was used as control for target siRNA, and the same sequence with Alexa-555 tag was used to determine uptake and distribution in tumor and other organs *in vivo*. *In vitro* transient transfection was performed as described previously (Landen et al., 2005).

DNA extraction and methylation analysis

Following DNA extraction, methylation analysis was done using a methylation kit (EZ-96 gold; Zymo Research, Orange, CA). MethPrimer software was used for the prediction of CpG island of Mm VASH1 and design of methylation specific primers (methylated VASH1 promoter: TTAGGGATTTACGTATCGACGT (forward); AAACGACAAACTCCAACCG (reverse); and unmethylated VASH1 promoter: TTTTTTTTAGGGATTTATGTATTGATGT (forward); CTAAACAACAAACTCCAACCACA (reverse). PCR conditions were 94°C for 5 min with hot start, then 94°C for 45 s, 56°C for 45 s, and 72°C for 45 s (40 cycles). Image analysis (Scion Image for Windows) was used for semi-quantitative measurement of methylated and unmethylated VASH1. Methylated VASH1 was normalized to unmethylated VASH1. The experiments were repeated 3 times.

Orthotopic *in vivo* model of ovarian cancer and tissue processing

Female athymic nude mice (NCR-nu) were purchased from the NCI-Frederick Cancer Research and Development Center (Frederick, MD) and maintained as previously described (Landen et al., 2005). All mouse studies were approved by the Institutional Animal Care and Use Committee. Mice were cared for in accordance with guidelines set forth by the American Association for Accreditation of Laboratory Animal Care and the US Public Health Service Policy on Human Care and Use of Laboratory Animals. For intra-ovarian injection, SKOV3ip1 cells (1×10^6) were injected directly into the left ovarian parenchyma through a left flank incision, as previously described (Lu et al., 2008). For therapy experiments, each siRNA was given twice weekly at a dose of 150 µg/kg body weight. At the time of sacrifice, mouse and tumor weight, number and distribution of tumors were recorded. Individuals who performed the necropsies were blinded to the treatment group assignments. Tissue specimens were fixed either with formalin, OCT; Miles, Inc., Elkhart, IN) or snap frozen in liquid nitrogen.

Immunofluorescence and confocal microscopy

Staining for EZH2, CD31, desmin, and ASMA was performed using frozen tissue as described previously (Lu et al., 2007b). Pericyte coverage was determined by the percent of vessels with 50% or more coverage of desmin-or ASMA-positive cells in 5 random fields at x200 magnification for each tumor.

Optical Imaging

Nude mice bearing HeyA8 tumors (i.p.) were given Cy 5.5 labeled siRNA/CH (n=5) or unlabeled siRNA/CH (n=6) i.v., or nothing (n=2). Forty-eight hours later, fluorescence imaging of excised tumor and organs was performed using the Xenogen IVIS 200 system. Cy5.5 fluorophore excitation ($\lambda_{\text{excitation}}=678$ nm) and emission ($\lambda_{\text{emission}}=703$ nm) filter sets were used. Using Living image 2.5 software, regions of interest (ROI) were drawn for each organ and total flux (photons/second or p/s) was measured as photons/s/cm²/steradian (p/s/cm²/Sr).

Western blot analysis

Western blot analysis was performed as previously reported (Halder et al., 2006; Landen et al., 2005).

Immunohistochemical staining

To quantify MVD in the mouse tumor samples, the number of blood vessels staining positive for CD31 (1:800 dilution, Pharmingen, San Diego, CA) was recorded in 10 random 0.159 mm² fields at x200 magnification (Thaker et al., 2006). All staining was quantified by 2 investigators in a blinded fashion. For human ovarian cancer samples, immunohistochemistry for EZH2 (1:400 dilution, Zymed, San Francisco, CA), CD34 (1:20 dilution, BioGenex Laboratories, San Ramon, CA (Ali-Fehmi et al., 2005; Des Guetz et al., 2006; Ino et al., 2006), VEGF (1:100 dilution, Santa Cruz Biotechnology, Inc., Santa Cruz, CA), desmin (1:200 dilution, Dako, Carpinteria, CA), ASMA (1:500 dilution, Abcam, Cambridge, MA), VASH1 (1:200 dilution, Abcam, Cambridge, MA), or NG2 (1:500 dilution, Santa Cruz Biotechnology Inc., Santa Cruz, CA) was performed, as described previously (Ali-Fehmi et al., 2005). For EZH2 and VEGF, the stained slides were scored by two investigators on the basis of the histochemical score (H-score; >100 defined as high expression and ≤ 100 , low expression), according to the method described by McCarty, et al. (Ali-Fehmi et al., 2005; McCarty et al., 1985; Merritt et al., 2008), which considers both the intensity of staining and the percentage of cells stained. MVD and pericyte coverage in clinical samples was quantified as described above.

Human ovarian cancer specimens

Following approval by the Institutional Review Board, 180 paraffin-embedded epithelial ovarian cancer specimens (collected between 1985 – 2004) with available clinical outcome data and confirmed diagnosis by a board-certified gynecologic pathologist were obtained from the Karmanos Cancer Institute tumor bank. The study was exempt from informed consent since it used previously collected residual tissue samples.

Statistical analysis

Differences in continuous variables were analyzed using the Mann-Whitney rank sum or t-test. The relationship between EZH2 expression and MVD was determined using the Wilcoxon ranked sums test. Statistical analyses were performed using SPSS 12.0 for Windows® (SPSS Inc., Chicago, IL). A 2-tailed $p < 0.05$ was considered statistically significant. Kaplan-Meier survival plots were generated and comparisons made using the

log-rank statistic. Bivariate orthogonal regression was used to describe the correlation between tumor and endothelial EZH2 expression (H-score).

Highlights

- EZH2 is a key regulator of tumor angiogenesis.
- VEGF stimulation increases EZH2 levels in endothelial cells.
- EZH2 silencing inhibits angiogenesis by activating VASH1.
- EZH2 targeting is an attractive therapeutic approach.

Supplementary Material

Refer to Web version on PubMed Central for supplementary material.

Acknowledgments

The authors thank Donna Reynolds, and Fang Wang for their technical expertise and helpful discussion. We also thank Dr. Vickie Williams for reviewing the manuscript. Portions of this work were supported by the NIH (CA 110793, 109298, P50 CA083639, P50 CA098258, CA128797, RC2GM092599), the Ovarian Cancer Research Fund, Inc. (Program Project Development Grant), the DOD (OC073399, W81XWH-10-1-0158, BC085265), NSC-96-3111-B, the Zarrow Foundation, the Marcus Foundation, and the Betty Anne Asche Murray Distinguished Professorship. WAS, AMN, ARC and RS are supported by NCI-DHHS-NIH T32 Training Grant (T32 CA101642). KM is supported by the GCF/OCRF Ann Schreiber Ovarian Cancer Research grant and an award from the Meyer and Ida Gordon Foundation #2. MMKS is supported by the NIH/NICHD WRHR Grant (HD050128) and the GCF-Molly Cade Ovarian Cancer Research Grant. MCH and LYL are supported by the #NSC 97-3111-B-039.

References

- Ali-Fehmi R, Morris RT, Bandyopadhyay S, Che M, Schimp V, Malone JM Jr, Munkarah AR. Expression of cyclooxygenase-2 in advanced stage ovarian serous carcinoma: correlation with tumor cell proliferation, apoptosis, angiogenesis, and survival. *Am J Obstet Gynecol.* 2005; 192:819–825. [PubMed: 15746677]
- Burger RA, Sill MW, Monk BJ, Greer BE, Sorosky JI. Phase II trial of bevacizumab in persistent or recurrent epithelial ovarian cancer or primary peritoneal cancer: a Gynecologic Oncology Group Study. *J Clin Oncol.* 2007; 25:5165–5171. [PubMed: 18024863]
- Burger RA, Brady MF, Bookman MA, Walker JL, Homesle HD, Fowler J, Monk BJ, Greer BE, Boente M, Liang SX. Phase III trial of bevacizumab (BEV) in the primary treatment of advanced epithelial ovarian cancer (EOC), primary peritoneal cancer (PPC), or fallopian tube cancer (FTC): a Gynecologic Oncology Group Study. *J Clin Oncol.* 2010; 28:7s.
- Cao R, Zhang Y. The functions of E(Z)/EZH2-mediated methylation of lysine 27 in histone H3. *Curr Opin Genet Dev.* 2004; 14:155–164. [PubMed: 15196462]
- Cavalli G, Paro R. Chromo-domain proteins: linking chromatin structure to epigenetic regulation. *Curr Opin Cell Biol.* 1998; 10:354–360. [PubMed: 9640536]
- Cha TL, Zhou BP, Xia W, Wu Y, Yang CC, Chen CT, Ping B, Otte AP, Hung MC. Akt-mediated phosphorylation of EZH2 suppresses methylation of lysine 27 in histone H3. *Science.* 2005; 310:306–310. [PubMed: 16224021]
- Chu CY, Chang CC, Prakash E, Kuo ML. Connective tissue growth factor (CTGF) and cancer progression. *J Biomed Sci.* 2008; 15:675–685. [PubMed: 18622762]
- Cicha I, Goppelt-Struebe M. Connective tissue growth factor: context-dependent functions and mechanisms of regulation. *Biofactors.* 2009; 35:200–208. [PubMed: 19449449]
- Des Guetz G, Uzzan B, Nicolas P, Cucherat M, Morere JF, Benamouzig R, Breau JL, Perret GY. Microvessel density and VEGF expression are prognostic factors in colorectal cancer. Meta-analysis of the literature. *Br J Cancer.* 2006; 94:1823–1832. [PubMed: 16773076]

- Donninger H, Bonome T, Radonovich M, Pise-Masison CA, Brady J, Shih JH, Barrett JC, Birrer MJ. Whole genome expression profiling of advance stage papillary serous ovarian cancer reveals activated pathways. *Oncogene*. 2004; 23:8065–8077. [PubMed: 15361855]
- Folkman J. What is the evidence that tumors are angiogenesis dependent? *J Natl Cancer Inst*. 1990; 82:4–6. [PubMed: 1688381]
- Halder J, Kamat AA, Landen CN Jr, Han LY, Lutgendorf SK, Lin YG, Merritt WM, Jennings NB, Chavez-Reyes A, Coleman RL, et al. Focal adhesion kinase targeting using in vivo short interfering RNA delivery in neutral liposomes for ovarian carcinoma therapy. *Clin Cancer Res*. 2006; 12:4916–4924. [PubMed: 16914580]
- Hosaka T, Kimura H, Heishi T, Suzuki Y, Miyashita H, Ohta H, Sonoda H, Moriya T, Suzuki S, Kondo T, Sato Y. Vasohibin-1 expression in endothelium of tumor blood vessels regulates angiogenesis. *Am J Pathol*. 2009; 175:430–439. [PubMed: 19498005]
- Howard KA, Rahbek UL, Liu X, Damgaard CK, Glud SZ, Andersen MO, Hovgaard MB, Schmitz A, Nyengaard JR, Besenbacher F, Kjems J. RNA interference in vitro and in vivo using a novel chitosan/siRNA nanoparticle system. *Mol Ther*. 2006; 14:476–484. [PubMed: 16829204]
- Huang J, Soffer SZ, Kim ES, McCrudden KW, New T, Manley CA, Middlesworth W, O’Toole K, Yamashiro DJ, Kandel JJ. Vascular remodeling marks tumors that recur during chronic suppression of angiogenesis. *Mol Cancer Res*. 2004; 2:36–42. [PubMed: 14757844]
- Ino K, Shibata K, Kajiyama H, Yamamoto E, Nagasaka T, Nawa A, Nomura S, Kikkawa F. Angiotensin II type 1 receptor expression in ovarian cancer and its correlation with tumour angiogenesis and patient survival. *Br J Cancer*. 2006; 94:552–560. [PubMed: 16434990]
- Jain RK, Duda DG, Clark JW, Loeffler JS. Lessons from phase III clinical trials on anti-VEGF therapy for cancer. *Nat Clin Pract Oncol*. 2006; 3:24–40. [PubMed: 16407877]
- Kamat AA, Kim TJ, Landen CN Jr, Lu C, Han LY, Lin YG, Merritt WM, Thaker PH, Gershenson DM, Bischoff FZ, et al. Metronomic chemotherapy enhances the efficacy of antivascular therapy in ovarian cancer. *Cancer Res*. 2007; 67:281–288. [PubMed: 17210709]
- Kerbel RS. Molecular and physiologic mechanisms of drug resistance in cancer: an overview. *Cancer Metastasis Rev*. 2001a; 20:1–2. [PubMed: 11831636]
- Kerbel RS, Yu J, Tran J, Man S, Vilorio-Petit A, Klement G, Coomber BL, Rak J. Possible mechanisms of acquired resistance to anti-angiogenic drugs: implications for the use of combination therapy approaches. *Cancer Metastasis Rev*. 2001b; 20:79–86. [PubMed: 11831651]
- Kern J, Steurer M, Gastl G, Günsilius E, Untergasser G. Vasohibin inhibits angiogenic sprouting in vitro and supports vascular maturation processes in vivo. *BMC Cancer*. 2009; 9:284. [PubMed: 19682397]
- Kidani K, Osaki M, Tamura T, Yamaga K, Shomori K, Ryoike K, Ito H. High expression of EZH2 is associated with tumor proliferation and prognosis in human oral squamous cell carcinomas. *Oral Oncol*. 2009; 45:39–46. [PubMed: 18619895]
- Kingston RE, Bunker CA, Imbalzano AN. Repression and activation by multiprotein complexes that alter chromatin structure. *Genes Dev*. 1996; 10:905–920. [PubMed: 8608939]
- Kleer CG, Cao Q, Varambally S, Shen R, Ota I, Tomlins SA, Ghosh D, Sewalt RG, Otte AP, Hayes DF, et al. EZH2 is a marker of aggressive breast cancer and promotes neoplastic transformation of breast epithelial cells. *Proc Natl Acad Sci U S A*. 2003; 100:11606–11611. [PubMed: 14500907]
- Kumar MNVR. A review of chitin and chitosan applications. *Reactive and Functional Polymers*. 2000; 46:1–27.
- Landen CN Jr, Chavez-Reyes A, Bucana C, Schmandt R, Deavers MT, Lopez-Berestein G, Sood AK. Therapeutic EphA2 gene targeting in vivo using neutral liposomal small interfering RNA delivery. *Cancer Res*. 2005; 65:6910–6918. [PubMed: 16061675]
- Langley RR, Ramirez KM, Tsan RZ, Van Arsdall M, Nilsson MB, Fidler IJ. Tissue-specific microvascular endothelial cell lines from H-2K(b)-tsA58 mice for studies of angiogenesis and metastasis. *Cancer Res*. 2003; 63:2971–2976. [PubMed: 12782605]
- Lu C, Bonome T, Li Y, Kamat AA, Han LY, Schmandt R, Coleman RL, Gershenson DM, Jaffe RB, Birrer MJ, Sood AK. Gene alterations identified by expression profiling in tumor-associated endothelial cells from invasive ovarian carcinoma. *Cancer Res*. 2007a; 67:1757–1768. [PubMed: 17308118]

- Lu C, Kamat AA, Lin YG, Merritt WM, Landen CN, Kim TJ, Spannuth W, Arumugam T, Han LY, Jennings NB, et al. Dual targeting of endothelial cells and pericytes in antivascular therapy for ovarian carcinoma. *Clin Cancer Res*. 2007b; 13:4209–4217. [PubMed: 17634550]
- Lu C, Thaker PH, Lin YG, Spannuth W, Landen CN, Merritt WM, Jennings NB, Langley RR, Gershenson DM, Yancopoulos GD, et al. Impact of vessel maturation on antiangiogenic therapy in ovarian cancer. *Am J Obstet Gynecol*. 2008; 198:477, e471–479. [PubMed: 18395047]
- Matsukawa Y, Semba S, Kato H, Ito A, Yanagihara K, Yokozaki H. Expression of the enhancer of zeste homolog 2 is correlated with poor prognosis in human gastric cancer. *Cancer Sci*. 2006; 97:484–491. [PubMed: 16734726]
- McCarty KS Jr, Miller LS, Cox EB, Konrath J, McCarty KS Sr. Estrogen receptor analyses. Correlation of biochemical and immunohistochemical methods using monoclonal antireceptor antibodies. *Arch Pathol Lab Med*. 1985; 109:716–721. [PubMed: 3893381]
- McGarvey KM, Greene E, Fahrner JA, Jenuwein T, Baylin SB. DNA methylation and complete transcriptional silencing of cancer genes persist after depletion of EZH2. *Cancer Res*. 2007; 67:5097–5102. [PubMed: 17545586]
- Merritt WM, Lin YG, Han LY, Kamat AA, Spannuth WA, Schmandt R, Urbauer D, Pennacchio LA, Cheng JF, Nick AM, et al. Dicer, Drosha, and outcomes in patients with ovarian cancer. *N Engl J Med*. 2008; 359:2641–2650. [PubMed: 19092150]
- Ptasinska A, Wang S, Zhang J, Wesley RA, Danner RL. Nitric oxide activation of peroxisome proliferator-activated receptor gamma through a p38 MAPK signaling pathway. *FASEB J*. 2007; 21:950–961. [PubMed: 17197391]
- Raman JD, Mongan NP, Tickoo SK, Boorjian SA, Scherr DS, Gudas LJ. Increased expression of the polycomb group gene, EZH2, in transitional cell carcinoma of the bladder. *Clin Cancer Res*. 2005; 11:8570–8576. [PubMed: 16361539]
- Relf M, LeJeune S, Scott PA, Fox S, Smith K, Leek R, Moghaddam A, Whitehouse R, Bicknell R, Harris AL. Expression of the angiogenic factors vascular endothelial cell growth factor, acidic and basic fibroblast growth factor, tumor growth factor beta-1, platelet-derived endothelial cell growth factor, placenta growth factor, and pleiotrophin in human primary breast cancer and its relation to angiogenesis. *Cancer Res*. 1997; 57:963–969. [PubMed: 9041202]
- Shen J, Yang X, Xiao WH, Hackett SF, Sato Y, Campochiaro PA. Vasohibin is up-regulated by VEGF in the retina and suppresses VEGF receptor 2 and retinal neovascularization. *FASEB J*. 2006; 20:723–725. [PubMed: 16473886]
- Simon J. Locking in stable states of gene expression: transcriptional control during *Drosophila* development. *Curr Opin Cell Biol*. 1995; 7:376–385. [PubMed: 7662368]
- Spannuth WA, Nick AM, Jennings NB, Armaiz-Pena GN, Mangala LS, Danes CG, Lin YG, Merritt WM, Thaker PH, Kamat AA, et al. Functional significance of VEGFR-2 on ovarian cancer cells. *Int J Cancer*. 2009; 124:1045–1053. [PubMed: 19058181]
- Spannuth WA, Sood AK, Coleman RL. Angiogenesis as a strategic target for ovarian cancer therapy. *Nat Clin Pract Oncol*. 2008; 5:194–204. [PubMed: 18268546]
- Stone RL, Sood AK, Coleman RL. Collateral damage: toxic effects of targeted antiangiogenic therapies in ovarian cancer. *Lancet Oncol*. 2010; 11:465–475. [PubMed: 20226736]
- Tamaki K, Moriya T, Sato Y, Ishida T, Maruo Y, Yoshinaga K, Ohuchi N, Sasano H. Vasohibin-1 in human breast carcinoma: a potential negative feedback regulator of angiogenesis. *Cancer Sci*. 2009; 100:88–94. [PubMed: 19037993]
- Thaker PH, Han LY, Kamat AA, Arevalo JM, Takahashi R, Lu C, Jennings NB, Armaiz-Pena G, Bankson JA, Ravoori M, et al. Chronic stress promotes tumor growth and angiogenesis in a mouse model of ovarian carcinoma. *Nat Med*. 2006; 12:939–944. [PubMed: 16862152]
- Tonini T, D'Andrilli G, Fucito A, Gaspa L, Bagella L. Importance of Ezh2 polycomb protein in tumorigenesis process interfering with the pathway of growth suppressive key elements. *J Cell Physiol*. 2008; 214:295–300. [PubMed: 17786943]
- Varambally S, Dhanasekaran SM, Zhou M, Barrette TR, Kumar-Sinha C, Sanda MG, Ghosh D, Pienta KJ, Sewalt RG, Otte AP, et al. The polycomb group protein EZH2 is involved in progression of prostate cancer. *Nature*. 2002; 419:624–629. [PubMed: 12374981]

- Watanabe K, Hasegawa Y, Yamashita H, Shimizu K, Ding Y, Abe M, Ohta H, Imagawa K, Hojo K, Maki H, et al. Vasohibin as an endothelium-derived negative feedback regulator of angiogenesis. *J Clin Invest.* 2004; 114:898–907. [PubMed: 15467828]
- Weikert S, Christoph F, Kollermann J, Muller M, Schrader M, Miller K, Krause H. Expression levels of the EZH2 polycomb transcriptional repressor correlate with aggressiveness and invasive potential of bladder carcinomas. *Int J Mol Med.* 2005; 16:349–353. [PubMed: 16012774]
- Wu ZL, Zheng SS, Li ZM, Qiao YY, Aau MY, Yu Q. Polycomb protein EZH2 regulates E2F1-dependent apoptosis through epigenetically modulating Bim expression. *Cell Death Differ.* 2010; 17:801–810. [PubMed: 19893569]
- Yoshinaga K, Ito K, Moriya T, Nagase S, Takano T, Niikura H, Yaegashi N, Sato Y. Expression of vasohibin as a novel endothelium-derived angiogenesis inhibitor in endometrial cancer. *Cancer Sci.* 2008; 99:914–919. [PubMed: 18325046]
- Zhu Y, Jin K, Mao XO, Greenberg DA. Vascular endothelial growth factor promotes proliferation of cortical neuron precursors by regulating E2F expression. *FASEB J.* 2003; 17:186–193. [PubMed: 12554697]

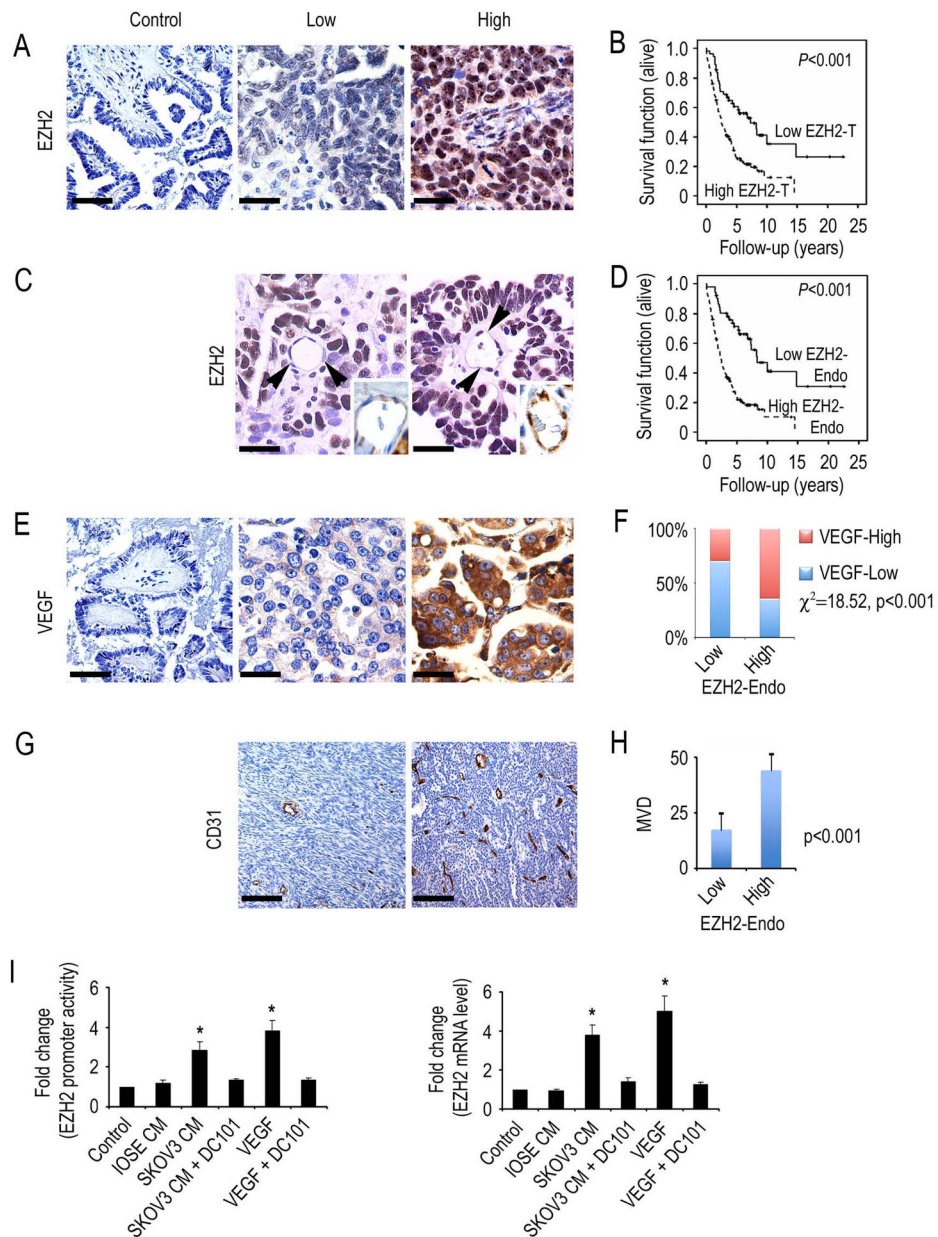


Figure 1. EZH2 expression in human ovarian carcinoma

(A) Representative images of human tumors with low and high EZH2 expression based on immunohistochemical staining. Scale bar = 50 μ m.

(B) Kaplan-Meier curves of disease-specific mortality for patients whose ovarian tumors expressed high or low levels of EZH2 (EZH2-T). The log-rank test (two-sided) was used to compare differences between the two groups. Increased EZH2-T was significantly associated with decreased overall survival ($p < 0.001$).

(C) Representative images of human ovarian cancer vasculature (arrowheads point to endothelial cells) with low or high immunohistochemical staining for EZH2. Scale bar = 25 μ m. Insets show blood vessels at higher magnification.

(D) Kaplan-Meier curves of disease-specific mortality of patients whose ovarian vasculature expressed low versus high EZH2 (EZH2-Endo). High EZH2-Endo expression was predictive of poor overall survival.

- (E) Representative images of human epithelial ovarian cancers with low or high immunohistochemical staining for VEGF. Scale bar = 50 μm .
- (F) VEGF expression was strongly associated with high EZH2-Endo expression levels.
- (G) Representative images of human ovarian cancers with low or high immunohistochemical staining for microvessel density (MVD). Scale bar = 100 μm .
- (H) Differences in mean MVD based on EZH2-Endo expression levels in human epithelial ovarian cancers.
- (I) VEGF increases EZH2 in endothelial cells. Results are in response to 6-hour treatment with VEGF (50 ng/mL), or conditioned medium (CM) from the non-cancerous ovarian epithelial cell line IOSE120, or the SKOV3 ovarian cancer cells. Fold changes represent the mean of triplicate experiments compared to untreated control cells. * $p < 0.01$. EZH2 promoter activity and mRNA levels are increased in mouse ovarian endothelial cells (MOEC) in response to VEGF, or conditioned media from ovarian cancer cells. Error bars indicate SD. See also Figure S1.

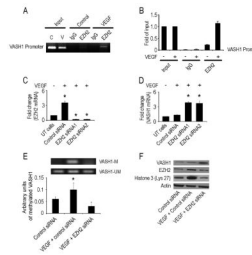


Figure 2. EZH2 gene silencing increases VASH1 mRNA expression in endothelial cells

(A) ChIP assay of EZH2 binding to VASH1 promoter in response to VEGF in mouse ovarian endothelial cells (MOEC). Cross-linked chromatin from MOEC was treated with (+) or without (-) VEGF and immunoprecipitated (IP) using EZH2 or mouse IgG antibodies. The input and immunoprecipitated DNA were subjected to PCR using primers corresponding to the 3800 to 3584 base pairs upstream of VASH1 transcription start site. PCR products were examined on ethidium bromide-stained agarose gel.

(B) Quantitative ChIP assay of EZH2 binding to VASH1 promoter in response to VEGF in endothelial cells. Treatment conditions are similar to those described in Panel A. PCR products were examined by Roche SYBR Green System for quantitative PCR.

(C) MOECs were transfected with control or mouse EZH2 siRNA (two different sequences) and harvested after 72 hours. Untransfected (UT) cells were used as controls. RNA was isolated and subjected to real-time quantitative RT-PCR. The fold difference represents the mean of triplicate experiments compared to control siRNA treated cells. * $p < 0.01$.

(D) Fold change in VASH1 mRNA levels in MOEC following transfection with either control or EZH2 siRNA (two different sequences). * $p < 0.01$.

(E) The effect of EZH2 gene silencing on VASH1 methylation in VEGF-treated MOECs was detected by methylation specific PCR. The inhibitory units of methylated VASH1 were normalized by that of the un-methylated VASH1 and represent the mean of triplicate experiments. * $p < 0.05$.

(F) Western blot of lysate collected 48 hours after transfection of MOEC with control, VEGF treated and mouse EZH2 siRNA treated cells.

Error bars indicate SEM.
See also Figure S2.

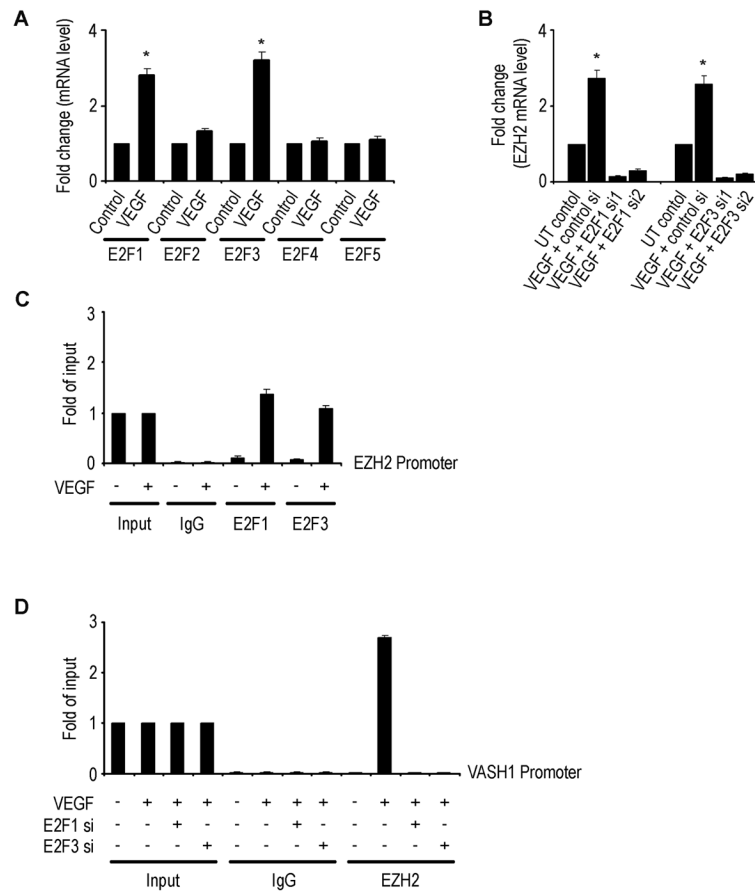


Figure 3. E2F mediated regulation of EZH2 and VASH1

(A) Expression levels of E2F transcription factors in mouse ovarian endothelial cells (MOEC) following treatment with VEGF. * $p < 0.01$.

(B) Effect of VEGF and either control, E2F1, or E2F3 siRNA (two different sequences) on EZH2 mRNA levels. The fold change in levels of mRNA expression represents the mean of triplicate experiments. * $p < 0.01$.

(C) Quantitative ChIP assay of E2F1 and E2F3 binding to EZH2 promoter in response to VEGF in MOEC. Crosslinked chromatin from MOECs treated with (+) or without (-) VEGF 50 ng/mL was immunoprecipitated using E2F1, E2F3, or mouse IgG antibodies. The input and immunoprecipitated DNA were subjected to PCR using primers corresponding to the 442 to 151 base pairs upstream of EZH2 transcription site. PCR products were examined by Roche SYBR Green System for quantitative PCR.

(D) Crosslinked chromatin from MOECs treated with (+) or without (-) indicated siRNA and with (+) or without (-) VEGF 50 ng/mL was immunoprecipitated using EZH2 or mouse IgG antibodies. The input and immunoprecipitated DNA were subjected to PCR using primers corresponding to the 3800 to 3584 base pairs upstream of VASH1 transcription site. PCR products were examined by Roche SYBR Green System for quantitative PCR.

Error bars indicate SEM.

See also Figure S3.

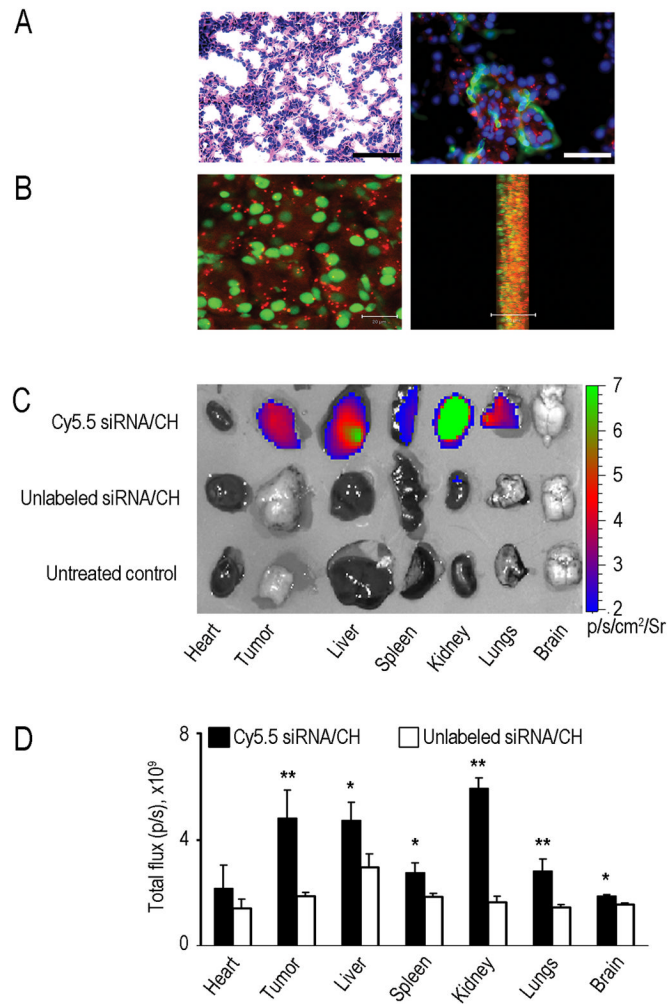


Figure 4. *In vivo* siRNA delivery using chitosan (CH) nanoparticles

Distribution of siRNA following single intravenous injection of Alexa-555 siRNA/CH nanoparticles in orthotopic HeyA8 tumor bearing nude mice. Fluorescent siRNA distribution in tumor tissue:

(A) Hematoxylin and eosin, original magnification x200 (left); tumor tissues were stained with anti-CD31 (green) antibody to detect endothelial cells (right). Scale bar = 50 μ m.

(B) Sections (8- μ m thick) were stained with sytox green and examined with confocal microscopy (scale bar 20 μ m) (left); lateral view (right). Photographs taken every 1 μ m were stacked and examined from the lateral view. Nuclei were labeled with sytox green and fluorescent siRNA (red) was seen throughout the section. At all time points, punctated emissions of the siRNA were noted in the perinuclear regions of individual cells, and siRNA was seen in >80% of fields examined.

(C–D) Optical imaging of organs and tumors from HeyA8 tumor-bearing mice treated with either Cy5.5 siRNA/CH or unlabeled siRNA/CH. (C) Fluorescence intensity overlaid on white light images of different mouse organs and tumor. (D) Semi-quantitative evaluation of fluorescence intensity in different mouse organs. Error bars indicate SD. * $p < 0.05$; ** $p < 0.01$.

See also Figure S4.

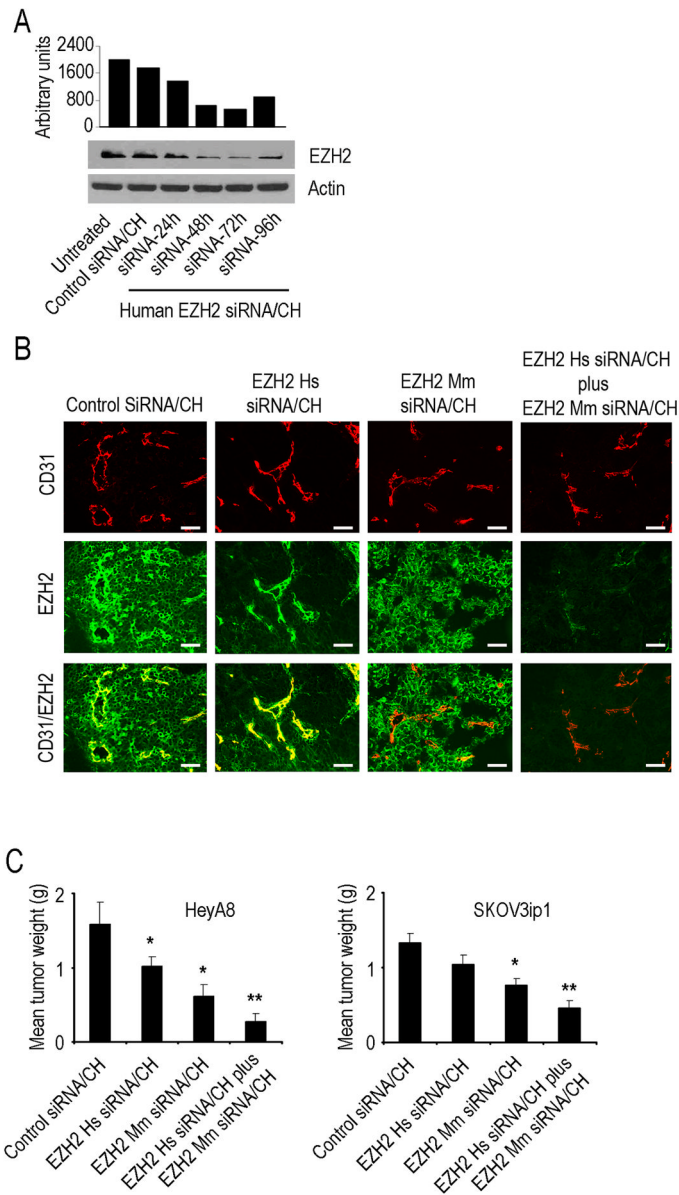


Figure 5. Effects of EZH2 gene silencing on *in vivo* ovarian cancer growth

(A) Western blot of lysates from orthotopic tumors collected 24, 48, 72 and 96 hours after a single injection of control siRNA/CH or human (EZH2 Hs siRNA/CH).

(B) EZH2 gene silencing in HeyA8 tumor as well as tumor endothelial cells. Tumors collected after 48 hours of single injection of control siRNA/CH, or EZH2 Hs siRNA/CH, or EZH2 Mm siRNA/CH and stained for EZH2 (green) and CD31 (red). Scale bar = 50 μ m.

(C) Effects of EZH2 Hs siRNA/CH or EZH2 Mm siRNA/CH on tumor weight in orthotopic mouse models of ovarian cancer. Error bars indicate SEM. * $p < 0.05$; ** $p < 0.001$. See also Table S1; Figure S5.

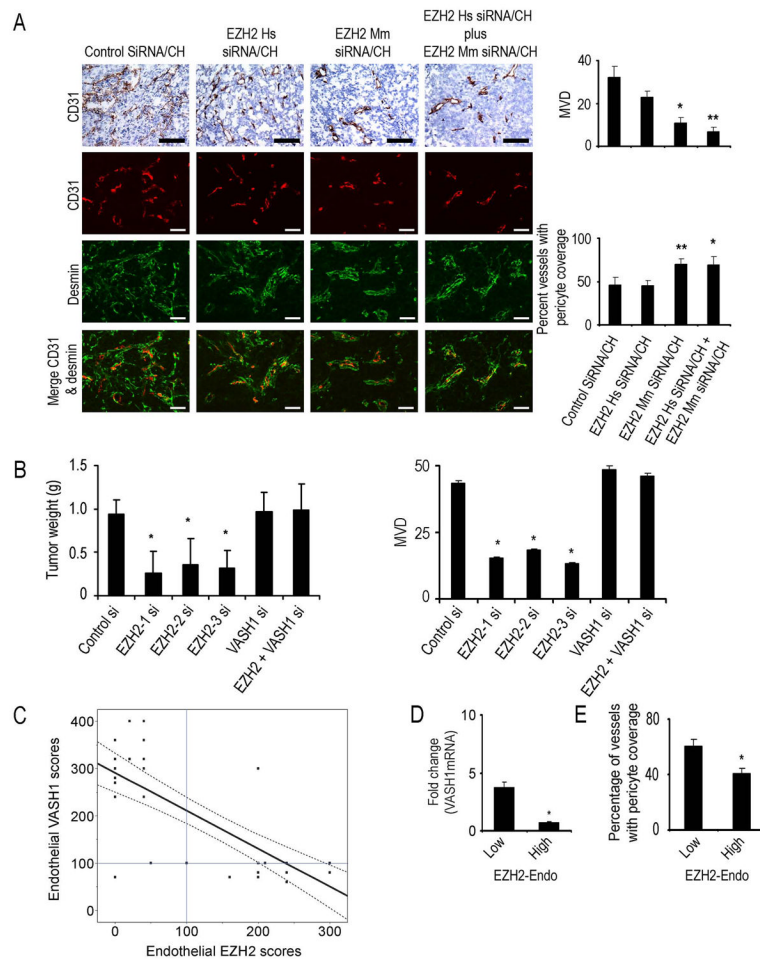


Figure 6. Effect of EZH2 targeting on tumor vasculature

(A) Effect of tumor (EZH2 Hs siRNA/CH) or endothelial (EZH2 Mm siRNA/CH) targeted EZH2 siRNA on microvessel density (MVD) and pericyte coverage. Tumors harvested following 4 to 5 weeks of therapy were stained for CD31 (MVD; red) and desmin (pericyte coverage; green). Scale bar = 50 μ m. The bars in the graphs correspond sequentially to the labeled columns of images at left. * $p < 0.01$; ** $p < 0.001$.

(B) Effects of VASH1 gene silencing on tumor growth *in vivo*. Nude mice injected with SKOV3ip1 ovarian cancer cells into the peritoneal cavity were randomly divided into 6 groups (10 mice per group): (1) control siRNA/CH (control si), (2) EZH2 Mm siRNA1/CH (EZH2-1 si), (3) EZH2 Mm siRNA2/CH (EZH2-2 si) (4) EZH2 Mm siRNA3/CH (EZH2-3 si) (5) VASH1 Mm siRNA1/CH (VASH1 si) and (6) combination of EZH2 Mm siRNA1/CH plus VASH1 Mm siRNA/CH. * $p < 0.05$. MVD is shown graphically in the adjacent graph.

(C) Endothelial VASH1 protein expression is plotted against endothelial EZH2 expression in 37 epithelial ovarian cancer specimens. The best-fit linear regression model is depicted with 95% confidence limits ($R^2 = -0.59$, $p < 0.001$). The linear lines intersecting with 100 on each axis represent predetermined cut-off values of “high” vs. “low” expression. The presence of EZH2 expression was associated with low expression of VASH1, which was otherwise elevated in the absence of or in the presence of low EZH2 expression.

(D) VASH1 mRNA levels were measured in endothelial cells isolated from normal ovarian (n=3), and epithelial ovarian cancer (n=10) samples using quantitative RT-PCR. The final

mRNA levels in the tumor endothelial cells were converted to ratios of decreased (>1) or increased (≤ 1) relative to levels of mRNA in normal ovarian endothelial cells (* $p < 0.01$). (E) Vessel maturation was examined by determining the extent of pericyte coverage in human epithelial ovarian cancer samples using an anti-alpha smooth muscle actin (ASMA) antibody. * $p < 0.01$.

Error bars indicate SEM.

See also Table S2; Figure S6.

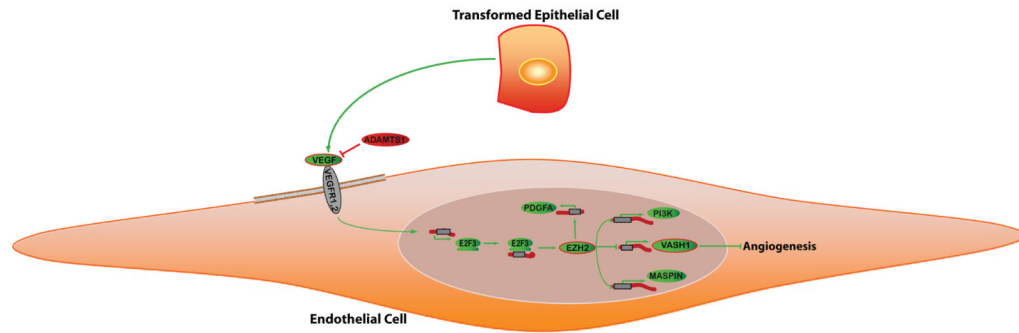


Figure 7.

Analysis of putative EZH2 pathways in cancer-associated endothelial cells. Pathway diagrams were generated with the assistance of Pathway Studio software (Ariadne, Rockville, MD). A model is reported in which VEGF stimulation leads to increased expression of E2F transcription factors, which directly modulates EZH2 levels. EZH2, a transcriptional repressor, causes VASH1 silencing by promoter methylation and subsequently increases angiogenesis.

Table 1

Association of clinical and demographic features with EZH2 in epithelial ovarian carcinoma

	EZH2-T overexpression		EZH2-Endo overexpression		p-value
	No	Yes	No	Yes	
Mean age	59.8 yrs (range 37-89 yrs)				
Stage					
Low (I/II)	20	9	20	9	
High (III-IV)	41	108	37	112	<0.001
Grade					
Low	9	7	10	6	
High	52	112	47	117	0.005
Histology					
Serous	39	100	35	104	
Other	22	18	22	18	<0.001